Int. J. Solids Structures Vol. 25, No. 2, pp. 129–149, 1989
Printed in Great Britain.

0020-7683/89 $3.00 + .00

ANALYSIS OF FREE DAMPED VIBRATION OF LAMINATED COMPOSITE PLATES AND SHELLS

ANDREW S. BICOS and GEORGE S. SPRINGER
Department of Aeronautics and Astronautics, Stanford University, Stanford, CA, U.S.A.

(*Received* 19 *March* 1988)

Abstract—Equations are derived which describe the free damped vibrations of plates and shells made of laminated fiber-reinforced, organic-matrix composites. A finite element method is developed for obtaining solutions to these equations. A computer code is written, which can be used to calculate the natural frequencies, mode shapes, and damping factors of rectangular plates, cylinders, and cylindrical panels with free, clamped, or simply supported edges, and with or without circular cutouts. Natural frequencies and mode shapes calculated by the code for isotropic and composite plates, cylinders, and cylindrical panels are compared with previous analytical, numerical, and experimental results. The results of the present study agree closely with those reported by previous investigators.

1. INTRODUCTION

In recent years, many analyses have been proposed for calculating the vibrational characteristics of plates and shells made of fiber-reinforced composites. Most of the previous analyses were concerned with the problem of free undamped vibration, and most were formulated using the Kirchoff-Love assumption thereby neglecting transverse shear deformation. Damping has been included by Alam and Asnani (1986), Lin *et al.* (1984), and Ni and Adams (1984) in their analyses of free vibrations of composite plates and beams, and by Alam and Asnani (1984a, b, 1987) in their analysis of free vibrations of circular cylinders made either of alternating layers of different isotropic materials or a specially orthotropic material. The effects of transverse shear strains have generally been considered only with reference to free vibrations of composite plates (Alam and Asnani, 1986, 1987; Lin *et al.*, 1984; Reddy, 1984; Phan and Reddy, 1985; Noor, 1972; Srinivas and Rao, 1970), with the apparent exception of Alam and Asnani's aforementioned study of a specially orthotropic cylinder.

Thus, the free vibration analyses of composite plates seem to be well in hand. However, corresponding analyses for shells, taking into account the effects of both damping and transverse shear strains, are not yet available. Therefore, the first objective of this investigation was to develop the equations describing the problem of free damped vibrations of composite shells, without introducing the Kirchoff–Love assumption. These results are presented in this paper. The second objective was to study the free damped vibrations of composite plates and shells containing circular cutouts. These results will be described in a forthcoming paper (Bicos and Springer, 1989).

2. PROBLEM STATEMENT

We consider a shell with principal radii of curvature R_1 and R_2 and thickness h (Fig. 1). The thickness h is small in comparison with the other dimensions of the shell. There are no forces or constraints applied on the upper or lower surfaces of the shell. Each outer edge of the shell may be clamped, simply supported, or free.

The shell is made of a laminated composite consisting of layers of unidirectional, continuous fibers embedded in an organic matrix. The layers are perfectly bonded. The shell may be made entirely of composite or of two composite face sheets enclosing a core, but the cross section must be symmetric with respect to the midsurface of the shell.

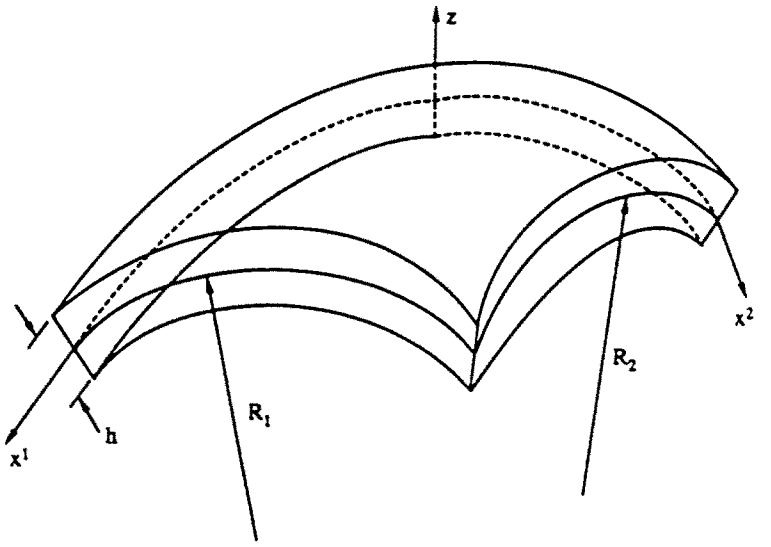

Fig. 1. Description of the shell.

The objective is to develop the equations which describe the free damped vibration of the shell, and can be used to calculate the natural frequencies, mode shapes, and damping factors.

3. GOVERNING EQUATIONS

In this section, the equations applicable to a general shell (Fig. 1) are presented in which: (a) the thickness h of the shell is small compared to all the other dimensions of the shell; (b) the thickness h is constant; (c) the material from which the shell is constructed is layered symmetrically with respect to the midsurface of the shell; and (d) each layer of the shell is either isotropic or orthotropic. The equations are developed on the basis of the following assumptions:

(1) the material from which the shell is constructed behaves in a linearly elastic manner;

(2) the material exhibits light damping, i.e. any vibration of the material dies out in an amount of time that is large in comparison to the period of vibration;

(3) damping of the material is independent of the frequency of the vibration (this assumption, although generally invalid for an isotropic metal, is often justified for fiber-reinforced organic matrix composites);

(4) the shell vibrations are simple harmonic motions;

(5) the effects of gravity on the vibration of the shell are negligible.

It is further assumed that the transverse normal stress σ_{zz} at any point is much smaller than any of the other stresses at that point and is, therefore, negligible. The component of the displacement normal to the shell midsurface ("out-of-plane" component with magnitude u_3) is assumed to be constant through the thickness. The displacement components perpendicular to the normal component of displacement ("in-plane" components) are assumed to vary through the thickness such that transverse shear strains are nonzero. The latter assumption implies that the Kirchhoff–Love assumption (Naghdi, 1963), that normals to the midsurface before deformation remain normal and straight after deformation, is not assumed in the present analysis.

After the governing equations have been derived we utilize a finite element method to generate numerical values of the natural frequencies, mode shapes, and damping factors. Because the resulting finite element formulation of the problem is very large, and because we are interested only in the first few eigenvalues and eigenvectors, the problem is attacked in two steps. In the first step, the undamped natural frequencies and the corresponding undamped mode shapes of the shell are obtained. For lightly damped structures, such as

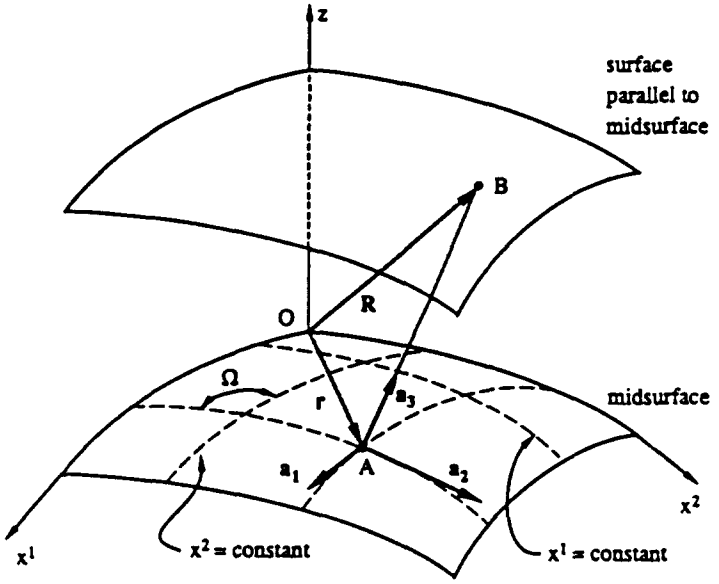

Fig. 2. Definition of the coordinate system and midsurface base vectors. For an orthogonal lines-of-curvature coordinate system, $\Omega = 90°$, and the coordinate lines (x^1 = constant and x^2 = constant) are identical to the lines of curvature.

those considered in this study, the undamped natural frequencies and mode shapes are nearly the same as the damped natural frequencies and mode shapes. In the second step, the damping corresponding to each mode of vibration, as expressed in terms of a modal damping factor, is calculated.

3.1. *Geometrical considerations*

In developing the governing equations we employed a general coordinate system shown in Fig. 2. The various components of vectors and tensors in this coordinate system can be found in texts, such as Naghdi (1963), and are not given here in detail. Only those aspects of the coordinate system are described which are needed in the subsequent analysis. A coordinate (x^1, x^2, z) attached to the shell midsurface is used. The base vectors $\{\mathbf{a}_1, \mathbf{a}_2, \mathbf{a}_3\}$, associated with the coordinate system shown in Fig. 2, satisfy the following conditions (Naghdi, 1963, 1984)

$$\mathbf{a}_\alpha = \mathbf{r}_{,\alpha} \tag{1}$$

$$\mathbf{a}_3 \cdot \mathbf{a}_3 = 1, \quad \mathbf{a}_\alpha \cdot \mathbf{a}_3 = 0, \quad \mathbf{a}_\alpha \cdot \mathbf{a}^\beta = \delta_\alpha^\beta, \quad \mathbf{a}_{3,\alpha} \cdot \mathbf{a}_3 = 0 \tag{2}$$

where δ_α^β is the Kronecker delta. The metric coefficients of the shell midsurface are given by

$$a_{\alpha\beta} = \mathbf{a}_\alpha \cdot \mathbf{a}_\beta. \tag{3}$$

Here, and in what follows, bold face type indicates a vector, a comma denotes partial differentiation, and subscripts α and β take on the values of 1 and 2. The vector $\mathbf{r}$ is the position vector of any point on the shell midsurface.

The position vector $\mathbf{R}$ of an arbitrary point B inside the shell is related to the position vector $\mathbf{r}$ of a corresponding point A on the shell midsurface by (Fig. 3)

$$\mathbf{R} = \mathbf{r} + z\mathbf{a}_3. \tag{4}$$

Any first, second, third, or fourth rank tensor evaluated at point B inside the shell can be expressed in terms of the components with respect to the base vectors $\{\mathbf{a}_1, \mathbf{a}_2, \mathbf{a}_3\}$ at point

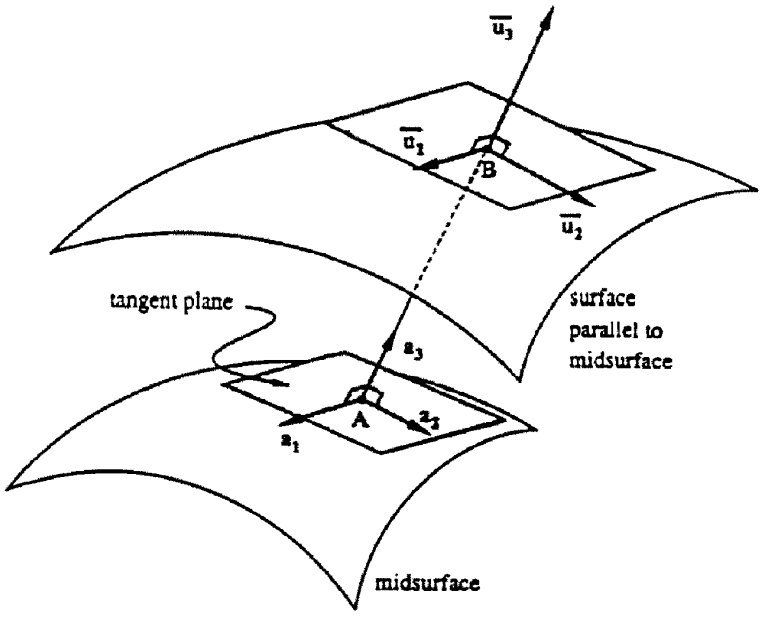

Fig. 3. Definition of the displacement vector components with respect to the shell midsurface.

A on the midsurface. The following expressions relate the components of a tensor with respect to the midsurface base vectors (Naghdi, 1984):

$$\text{first rank} \quad [\bar{T}^{\alpha}]\mathbf{a}_{\alpha} = \mu^{\alpha}_{\beta}[T^{\beta}]\mathbf{a}_{\alpha} \tag{5}$$

$$\text{second rank} \quad [\bar{T}^{\alpha\beta}]\mathbf{a}_{\alpha} \otimes \mathbf{a}_{\beta} = \mu^{\alpha}_{\sigma}\mu^{\beta}_{\gamma}[T^{\sigma\gamma}]\mathbf{a}_{\alpha} \otimes \mathbf{a}_{\beta} \tag{6}$$

$$\text{third rank} \quad [\bar{T}^{\alpha\beta\gamma}]\mathbf{a}_{\alpha} \otimes \mathbf{a}_{\beta} \otimes \mathbf{a}_{\gamma} = \mu^{\alpha}_{\sigma}\mu^{\beta}_{\delta}\mu^{\gamma}_{\omega}[T^{\sigma\delta\omega}]\mathbf{a}_{\alpha} \otimes \mathbf{a}_{\beta} \otimes \mathbf{a}_{\gamma} \tag{7}$$

$$\text{fourth rank} \quad [\bar{T}^{\alpha\beta\gamma\delta}]\mathbf{a}_{\alpha} \otimes \mathbf{a}_{\beta} \otimes \mathbf{a}_{\gamma} \otimes \mathbf{a}_{\delta} = \mu^{\alpha}_{\sigma}\mu^{\beta}_{\nu}\mu^{\gamma}_{\omega}\mu^{\delta}_{\omega}[T^{\sigma\nu\omega\omega}]\mathbf{a}_{\alpha} \otimes \mathbf{a}_{\beta} \otimes \mathbf{a}_{\gamma} \otimes \mathbf{a}_{\delta} \tag{8}$$

where $\otimes$ is the tensor product symbol and

$$\mu^{\beta}_{\alpha} = \delta^{\beta}_{\alpha} - zb^{\beta}_{\alpha}. \tag{9}$$

b^{β}_{α} are the coefficients of the curvature tensor. The terms in brackets on the right-hand side of eqns (5)–(8) are referred to as the coefficients of the tensor at point B and the terms in brackets on the left-hand side of these equations are referred to as the coefficients of the tensor with respect to the midsurface base vectors at point A.

For the orthogonal lines-of-curvature coordinate system, the curvature coefficients are (Naghdi, 1963)

$$b^1_1 = -\frac{1}{R_1}, \quad b^2_2 = -\frac{1}{R_2}, \quad b^2_1 = b^1_2 = 0. \tag{10}$$

Regarding the notation used in eqns (1)–(9), the following comments are made. In these equations, as well as in all subsequent analysis, subscripts denote covariant tensor coefficients and superscripts denote contravariant tensor coefficients (Flugge, 1972). Furthermore, all Greek indices (subscripts and superscripts) take on the values of 1 and 2. Lastly, summation is implied whenever a subscript and superscript have the same index in an expression.

3.2. *Kinematics*

The analysis which follows is along the lines presented by Reddy (1984) for composite plates. For the coordinate system shown in Fig. 2 and discussed above, the coefficients of the strain tensor at any point in the shell are (Naghdi, 1963)

$$e_{\alpha\beta} = \tfrac{1}{2}\mu^{\gamma}_{\alpha}(\bar{u}_{\gamma|\beta} - b_{\gamma\beta}\bar{u}_3) + \tfrac{1}{2}\mu^{\gamma}_{\beta}(\bar{u}_{\gamma|\alpha} - b_{\gamma\alpha}\bar{u}_3) \tag{11}$$

$$e_{\alpha 3} = \tfrac{1}{2}(\mu^{\gamma}_{\alpha}\bar{u}_{\gamma,3} + \bar{u}_{3,\alpha} + b^{\gamma}_{\alpha}\bar{u}_{\gamma}) \tag{12}$$

$$e_{33} = \bar{u}_{3,3} \tag{13}$$

where $|$ denotes covariant differentiation with respect to base vectors $\{\mathbf{a}_1, \mathbf{a}_2, \mathbf{a}_3\}$, $\bar{u}_\gamma$ are the coefficients of the displacement vector components tangential to the surface at point B. These components, called intrinsic components, are in the plane tangent to the surface at point B (Fig. 3). $\bar{u}_3$ is the coefficient of the "out-of-plane" or normal component of the displacement vector at point B, called the extrinsic component of the displacement, and is normal to the plane tangent to the surface at point B.

The coefficients of the tangential or intrinsic components of the displacement vector are assumed to vary with position through the thickness according to the expression

$$\bar{u}_\alpha = v_\alpha + z\beta_\alpha + z^2\varphi_\alpha + z^3\psi_\alpha. \tag{14}$$

The coefficient of the normal or extrinsic component of the displacement vector is assumed to be constant through the thickness

$$\bar{u}_3 = w. \tag{15}$$

v_α, w, β_α, φ_α, and ψ_α are as yet undetermined displacement measures. These measures are functions of position $\mathbf{r}$ and time t.

The expression for the tangential displacement coefficients $\bar{u}_\alpha$ can be simplified by making use of the fact that the transverse shear stresses are zero on the load-free upper and lower surfaces of the shell (Reddy, 1984)

$$\sigma_{13} = \sigma_{23} = 0 \quad \text{at} \quad z = \pm\frac{h}{2}. \tag{16}$$

For shells constructed of isotropic or orthotropic layers, when the transverse shear stresses are zero on the outer surfaces, the transverse shear strains are also zero on these surfaces (Reddy, 1984)

$$e_{13} = e_{23} = 0 \quad \text{at} \quad z = \pm\frac{h}{2}. \tag{17}$$

By substituting eqns (14) and (15) into eqn (12) and making use of eqn (17), we obtain

$$\psi_\alpha = -\frac{4}{3h^2}\left(-\frac{h^2}{4}b^{\gamma}_{\alpha}\varphi_\gamma + \beta_\alpha + b^{\gamma}_{\alpha}v_\gamma + w_{,\alpha}\right) \tag{18}$$

$$\varphi_\alpha = \frac{h^2}{4}b^{\gamma}_{\alpha}\psi_\gamma. \tag{19}$$

For a plate the curvature coefficients b^{β}_{α} are zero and hence eqns (18) and (19) reduce to

$$\psi_\alpha = -\frac{4}{3h^2}(\beta_\alpha + w_{,\alpha}) \tag{20}$$

$$\varphi_\alpha = 0. \tag{21}$$

Table 1. Definitions of the strain measures

$\gamma_{\alpha\beta} = v_{\alpha\|\beta} - b_{\alpha\beta} w$	$\gamma_{\alpha 3} = \beta_\alpha + w_{,\alpha} + b_\alpha^\gamma v_\gamma$
$\kappa_{\alpha\beta} = \beta_{\alpha\|\beta}$	$\kappa_{\alpha 3} = -\frac{h^2}{2} b_\alpha^\gamma \psi_\gamma$
$\lambda_{\alpha\beta} = \frac{h^2}{4}(b_\alpha^\gamma \psi_\gamma)_{\|\beta}$	$\lambda_{\alpha 3} = 3\left(\delta_\alpha^\gamma - \frac{h^2}{12} b_\alpha^\gamma b_\sigma^\gamma\right)\psi_\gamma$
$\theta_{\alpha\beta} = \psi_{\alpha\|\beta}$	$\theta_{\alpha 3} = -2 b_\alpha^\gamma \psi_\gamma$

Equations (20) and (21) are the same as those derived by Reddy (1984) for a plate.

By substituting eqn (19) into eqn (14) we obtain

$$\bar{u}_\alpha = v_\alpha + z\beta_\alpha + z^2 \frac{h^2}{4} b_\alpha^\gamma \psi_\gamma + z^3 \psi_\alpha \tag{22}$$

where ψ_α are given by eqn (18).

In the following analysis, we will use eqn (22) to represent the coefficients of the tangential or intrinsic components of the displacement. This is in contrast to the often used method, where only a linear variation through the thickness is used to describe $\bar{u}_\alpha$ (Naghdi, 1984)

$$\bar{u}_\alpha = v_\alpha + z\beta_\alpha. \tag{23}$$

In our discussions we will refer to results obtained from eqn (22) as being of the "higher-order" theory and to results obtained from eqn (23) as being of the "standard" theory.

The coefficients of the strain tensor can now be expressed in terms of the unknown displacement measures v_α, w, β_α and ψ_α. By substituting eqns (15) and (22) into eqns (11) (13) we obtain

$$e_{\alpha\beta} = \tfrac{1}{2}\mu_\alpha^\gamma(\gamma_{\gamma\beta} + z\kappa_{\gamma\beta} + z^2\lambda_{\gamma\beta} + z^3\theta_{\gamma\beta}) + \tfrac{1}{2}\mu_\beta^\gamma(\gamma_{\gamma\alpha} + z\kappa_{\gamma\alpha} + z^2\lambda_{\gamma\alpha} + z^3\theta_{\gamma\alpha}) \tag{24}$$

$$e_{\alpha 3} = \tfrac{1}{2}(\gamma_{\alpha 3} + z\kappa_{\alpha 3} + z^2\lambda_{\alpha 3} + z^3\theta_{\alpha 3}) \tag{25}$$

$$e_{33} = 0 \tag{26}$$

where the tensor coefficients expressed in terms of the Greek letters represent the strain measures defined in Table 1. The four strain measures in the left-hand column correspond to the tangential or "in-plane" strains. The four strain measures in the right-hand column correspond to the transverse shear strains.

Three of the strain measures in Table 1 ($\gamma_{\alpha\beta}$, $\kappa_{\alpha\beta}$, and $\gamma_{\alpha 3}$) are the same as those that would be obtained using eqn (23) ("standard" theory (Naghdi, 1984)). The remaining five strain measures ($\lambda_{\alpha\beta}$, $\theta_{\alpha\beta}$, $\kappa_{\alpha 3}$, $\lambda_{\alpha 3}$, and $\theta_{\alpha 3}$) are due to the quadratic and cubic terms in eqn (22). Finally, for a plate in which the curvature coefficients b_α^β are zero, the equations in Table 1 reduce to the expression obtained by Reddy for a plate (Reddy, 1984).

3.3. *Constitutive relations*

The shell is made of isotropic or orthotropic layers (called plies or laminae). The properties of each layer are taken to be symmetric about the layer's midsurface (monoclinic material). The constitutive relations applicable to each layer are (Naghdi, 1963)

$$\sigma^{\alpha\beta} = C^{\alpha\beta\gamma\delta} e_{\gamma\delta} + C^{\alpha\beta 33} e_{33} \tag{27}$$

$$\sigma^{\alpha 3} = 2C^{\alpha 3\gamma 3} e_{\gamma 3} \tag{28}$$

$$\sigma^{33} = C^{33\gamma\delta} e_{\gamma\delta} + C^{3333} e_{33} \tag{29}$$

Table 2. Definitions of the stress resultants

$$N^{\alpha\beta} = \int_{-h/2}^{h/2} \mu\sigma^{\alpha\gamma}\mu_{\gamma}^{\beta}\,dz \qquad Q^{\alpha 3} = \int_{-h/2}^{h/2} \mu\sigma^{\alpha 3}\,dz$$

$$M^{\alpha\beta} = \int_{-h/2}^{h/2} \mu\sigma^{\alpha\gamma}\mu_{\gamma}^{\beta} z\,dz \qquad R^{\alpha 3} = \int_{-h/2}^{h/2} \mu\sigma^{\alpha 3} z\,dz$$

$$L^{\alpha\beta} = \int_{-h/2}^{h/2} \mu\sigma^{\alpha\gamma}\mu_{\gamma}^{\beta} z^2\,dz \qquad S^{\alpha 3} = \int_{-h/2}^{h/2} \mu\sigma^{\alpha 3} z^2\,dz$$

$$P^{\alpha\beta} = \int_{-h/2}^{h/2} \mu\sigma^{\alpha\gamma}\mu_{\gamma}^{\beta} z^3\,dz \qquad T^{\alpha 3} = \int_{-h/2}^{h/2} \mu\sigma^{\alpha 3} z^3\,dz$$

μ is defined by eqn (36).

where $\sigma^{\alpha\beta}$, $\sigma^{\alpha 3}$, and σ^{33} denote the coefficients of the stress tensor at any point, and $C^{\alpha\beta\gamma\delta}$, $C^{\alpha 3\gamma 3}$, $C^{\alpha\beta 33}$, $C^{33\gamma\delta}$, and C^{3333} are the coefficients of the elastic stiffness tensor (moduli tensor).

As stated previously, the transverse normal coefficient of stress σ^{33} is assumed to be negligible. Accordingly, eqns (27)–(29) become

$$\sigma^{\alpha\beta} = Q^{\alpha\beta\gamma\delta} e_{\gamma\delta}; \quad \sigma^{\alpha 3} = 2Q^{\alpha 3\gamma 3} e_{\gamma 3} \tag{30}$$

where $Q^{\alpha\beta\gamma\delta}$ and $Q^{\alpha 3\gamma 3}$ are the coefficients of the reduced stiffness tensor, defined as

$$Q^{\alpha\beta\gamma\delta} = C^{\alpha\beta\gamma\delta} - \frac{C^{\alpha\beta 33} C^{33\gamma\delta}}{C^{3333}}; \quad Q^{\alpha 3\gamma 3} = C^{\alpha 3\gamma 3}. \tag{31}$$

For orthotropic materials, the physical coefficients of the reduced stiffness tensor, in terms of the engineering constants, are given in Bicos (1987).

The aforementioned equations apply to a single ply or layer. For a laminate composed of several layers, the stress–strain relations can conveniently be expressed in terms of the stress resultants defined in Table 2.

By combining the aforementioned equations we obtain the constitutive relations for the laminate given in Table 3. For a plate, where the curvatures are zero, ${}_0B^{\alpha\beta\gamma\delta}$, ${}_1B^{\alpha\beta\gamma\delta}$,

Table 3. Laminate constitutive relations

$$N^{\alpha\beta} = {}_0B^{\alpha\beta\gamma\delta}\gamma_{\gamma\delta} + {}_1B^{\alpha\beta\gamma\delta}\kappa_{\gamma\delta} + {}_2B^{\alpha\beta\gamma\delta}\lambda_{\gamma\delta} + {}_3B^{\alpha\beta\gamma\delta}\theta_{\gamma\delta}$$

$$M^{\alpha\beta} = {}_1B^{\alpha\beta\gamma\delta}\gamma_{\gamma\delta} + {}_2B^{\alpha\beta\gamma\delta}\kappa_{\gamma\delta} + {}_3B^{\alpha\beta\gamma\delta}\lambda_{\gamma\delta} + {}_4B^{\alpha\beta\gamma\delta}\theta_{\gamma\delta}$$

$$L^{\alpha\beta} = {}_2B^{\alpha\beta\gamma\delta}\gamma_{\gamma\delta} + {}_3B^{\alpha\beta\gamma\delta}\kappa_{\gamma\delta} + {}_4B^{\alpha\beta\gamma\delta}\lambda_{\gamma\delta} + {}_5B^{\alpha\beta\gamma\delta}\theta_{\gamma\delta}$$

$$P^{\alpha\beta} = {}_3B^{\alpha\beta\gamma\delta}\gamma_{\gamma\delta} + {}_4B^{\alpha\beta\gamma\delta}\kappa_{\gamma\delta} + {}_5B^{\alpha\beta\gamma\delta}\lambda_{\gamma\delta} + {}_6B^{\alpha\beta\gamma\delta}\theta_{\gamma\delta}$$

$$Q^{\alpha 3} = {}_0B^{\alpha 3\gamma 3}\gamma_{\gamma 3} + {}_1B^{\alpha 3\gamma 3}\kappa_{\gamma 3} + {}_2B^{\alpha 3\gamma 3}\lambda_{\gamma 3} + {}_3B^{\alpha 3\gamma 3}\theta_{\gamma 3}$$

$$R^{\alpha 3} = {}_1B^{\alpha 3\gamma 3}\gamma_{\gamma 3} + {}_2B^{\alpha 3\gamma 3}\kappa_{\gamma 3} + {}_3B^{\alpha 3\gamma 3}\lambda_{\gamma 3} + {}_4B^{\alpha 3\gamma 3}\theta_{\gamma 3}$$

$$S^{\alpha 3} = {}_2B^{\alpha 3\gamma 3}\gamma_{\gamma 3} + {}_3B^{\alpha 3\gamma 3}\kappa_{\gamma 3} + {}_4B^{\alpha 3\gamma 3}\lambda_{\gamma 3} + {}_5B^{\alpha 3\gamma 3}\theta_{\gamma 3}$$

$$T^{\alpha 3} = {}_3B^{\alpha 3\gamma 3}\gamma_{\gamma 3} + {}_4B^{\alpha 3\gamma 3}\kappa_{\gamma 3} + {}_5B^{\alpha 3\gamma 3}\lambda_{\gamma 3} + {}_6B^{\alpha 3\gamma 3}\theta_{\gamma 3}$$

where

$${}_nB^{\alpha\beta\gamma\delta} = \int_{-h/2}^{h/2} \bar{Q}^{\alpha\beta\gamma\sigma}(\mu^{-1})_{\mu}^{\beta}(\mu^{-1})_{\sigma}^{\delta}\mu z^n\,dz, \quad n = 0, 1, \ldots, 6$$

$${}_nB^{\alpha 3\gamma 3} = \int_{-h/2}^{h/2} \bar{Q}^{\alpha 3\gamma 3}(\mu^{-1})_{\mu}^{\gamma}(\mu^{-1})_{\sigma}^{\gamma}\mu z^n\,dz, \quad n = 0, 1, \ldots, 6$$

and $\bar{Q}^{\alpha\beta\gamma\sigma}$ and $\bar{Q}^{\alpha 3\gamma 3}$ are the coefficients of the reduced stiffness tensor with respect to the midsurface and $(\mu^{-1})_{\gamma}^{\beta}$ is the inverse of μ_{γ}^{β}.

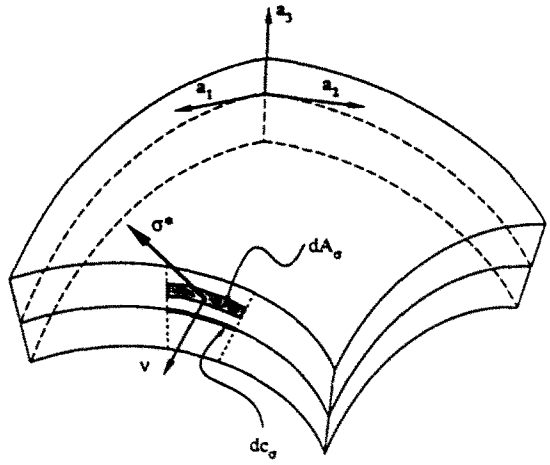

Fig. 4. Illustration of an edge element and edge traction.

and ${}_2B^{\alpha\beta\gamma\delta}$ become the in-plane, in-plane/bending coupling, and bending stiffness tensors, respectively. These tensors are identical to the $A^{\alpha\beta\gamma\delta}$, $B^{\alpha\beta\gamma\delta}$, and $D^{\alpha\beta\gamma\delta}$ tensors used in conventional laminate plate theory (Tsai and Hahn, 1980; Jones, 1975).

In Tables 2 and 3, $N^{\alpha\beta}$, $M^{\alpha\beta}$, and $Q^{\alpha 3}$ are the tangential or membrane stress resultants, moment resultants, and transverse shear stress resultants, respectively. These three resultants are identical to those of the "standard" theory, in which the tangential coefficients of the displacement $\bar{u}_\alpha$ are assumed to vary linearly through the thickness (eqn (23)). The additional resultant tensors given in Table 2 do not appear in the "standard" theory; they arise here due to the higher-order terms in our approximation for $\bar{u}_\alpha$ (eqn (22)).

3.4. *Equations of motion*

The equations of motion are derived using the extended Hamilton's principle (Meirovitch, 1967). For the shell under consideration, the extended Hamilton's principle takes the form of

$$\delta \int_{t_1}^{t_2} \left[\iiint_V (T - \hat{U})\, \mathrm{d}V + \iint_{A_\sigma} (\sigma^{*\alpha\beta} \nu_\beta \mu_\alpha^\gamma \bar{u}_\gamma + \sigma^{*3\beta} \nu_\beta \bar{u}_3)\, \mathrm{d}A_\sigma \right] \mathrm{d}t = 0 \tag{32}$$

where δ is the variation symbol, and t_1 and t_2 are two instants of time. T is the kinetic energy density

$$T = \tfrac{1}{2}\rho(\dot{\bar{u}}^\alpha \dot{\bar{u}}_\alpha + \dot{w}^2) \tag{33}$$

where ρ is the material density and dots indicate differentiation with respect to time. $\hat{U}$ is the strain energy density

$$\hat{U} = \tfrac{1}{2} Q^{\alpha\beta\gamma\delta} e_{\alpha\beta} e_{\gamma\delta} + 2Q^{\alpha 3\gamma 3} e_{\alpha 3} e_{\gamma 3}. \tag{34}$$

V is the volume of the shell and $\mathrm{d}V$ is a volume element

$$\mathrm{d}V = \mu\, \mathrm{d}z\, \mathrm{d}A_\alpha \tag{35}$$

where μ is the determinant of μ_α^β given by

$$\mu = 1 - 2zH + z^2 K. \tag{36}$$

H is the mean curvature and K the Gaussian curvature of the midsurface

$$H = -\frac{1}{2}\left(\frac{1}{R_1} + \frac{1}{R_2}\right); \quad K = \frac{1}{R_1 R_2}. \tag{37}$$

dA_σ is a midsurface area element. A_σ is the edge area on which the applied stresses are specified, and dA_σ is an element along this edge (Fig. 4)

$$v_\beta \, dA_\sigma = \bar{v}_\beta \mu \, dz \, dc_\sigma \tag{38}$$

where dc_σ is the corresponding midsurface edge line element, v_β the components of the unit normal vector at a point off the midsurface, and $\bar{v}_\beta$ the components of this unit normal vector with respect to the midsurface. $\sigma^{*z\beta}$ and $\sigma^{*3\beta}$ are the stress components corresponding to the specified edge tractions.

By combining eqns (15)–(38) together with those in Tables 1–3, after very lengthy but straightforward calculations (Bicos, 1987), we obtain the equations that describe the motion of the shell. The resulting equations are listed in Table 4 for orthogonal lines-of-curvature coordinates (Fig. 2). The first four equations apply at every point in the midsurface. The boundary conditions apply to points along the edge of the midsurface.

The displacement measures ψ_γ and the stress resultant tensors $L^{z\beta}$, $P^{z\beta}$, R^{z3}, S^{z3}, and T^{z3} appearing in the equations of motion are the result of the higher-order approximation employed here, i.e. they result from the quadratic and cubic terms included in the expression for the displacement $\bar{u}_\gamma$ (eqn (22)). By setting ψ_γ equal to zero in eqn (22), the equations of motion become identical to those that would be obtained if the "standard" approximation for $\bar{u}_\gamma$ (eqn (23)) were used.

The boundary conditions in Table 4 express the conditions that must be satisfied along the edge of the shell. These relations show that along an edge the following conditions must be specified:

Table 4. Equations of motion and boundary conditions

Orthogonal lines-of-curvature coordinate system (Fig. 2).

Equations of motion

$$-\left[I_0\ddot{e}_\alpha + I_1\ddot{\beta}_\alpha + \left(I_2\frac{h^2}{4}b_\alpha^\gamma + I_1\delta_\alpha^\gamma\right)\ddot{\psi}_\gamma\right]a^{\alpha\beta} + N_{||\alpha}^{\alpha\beta} - b_\alpha^\beta Q^{\alpha 3} = 0$$

$$-I_0\ddot{w} + b_{\alpha\beta}N^{\beta\alpha} + Q_{||\alpha}^{\alpha 3} = 0$$

$$-\left[I_1\ddot{e}_\alpha + I_2\ddot{\beta}_\alpha + \left(I_3\frac{h^2}{4}b_\alpha^\gamma + I_4\delta_\alpha^\gamma\right)\ddot{\psi}_\gamma\right]a^{\alpha\beta} + M_{||\alpha}^{\alpha\beta} - Q^{\alpha 3} = 0$$

$$-\left[\left(I_2\frac{h^2}{4}b_\gamma^\beta a^{\gamma\alpha} + I_1 a^{\alpha\beta}\right)\ddot{e}_\alpha + \left(I_3\frac{h^2}{4}b_\gamma^\beta a^{\gamma\alpha} + I_4 a^{\alpha\beta}\right)\ddot{\beta}_\alpha + \left(I_4\frac{h^4}{16}b_\gamma^\beta b_\alpha^\lambda a^{\lambda\alpha} + I_3\frac{h^2}{4}(b_\gamma^\lambda a^{\beta\alpha} + b_\alpha^\beta a^{\gamma\alpha}) + I_2 a^{\gamma\alpha}\right)\ddot{\psi}_\gamma\right] + \frac{h^2}{4}b_\gamma^\beta L_{||\alpha}^{\gamma\alpha} + P_{||\alpha}^{\beta\alpha} - \frac{h^2}{2}b_\alpha^\beta R^{\alpha 3} - 3\left(\delta_\alpha^\beta - \frac{h^2}{12}b_\alpha^\gamma b_\gamma^\beta\right)S^{\alpha 3} - 2b_\alpha^\beta T^{\alpha 3} = 0.$$

Boundary conditions

$$v_\alpha N^{\alpha\beta} = v_\alpha N^{*\alpha\beta} \quad \text{or} \quad \delta v_\beta = 0$$

and

$$v_\alpha M^{\alpha\beta} = v_\alpha M^{*\alpha\beta} \quad \text{or} \quad \delta\beta_\beta = 0$$

and

$$v_\alpha Q^{\alpha 3} = v_\alpha Q^{*\alpha 3} \quad \text{or} \quad \delta w = 0$$

and

$$v_\alpha\left(\frac{h^2}{4}b_\gamma^\beta L^{\gamma\alpha} + P^{\alpha\beta}\right) = v_\alpha\left(\frac{h^2}{4}b_\gamma^\beta L^{*\gamma\alpha} + P^{*\alpha\beta}\right) \quad \text{or} \quad \delta\psi_\beta = 0$$

where v_α are the components of the edge unit normal, and

$$I_n = \int_{-h/2}^{h/2} \rho\mu z^n \, dz, \quad n = 0, 1, \ldots, 6.$$

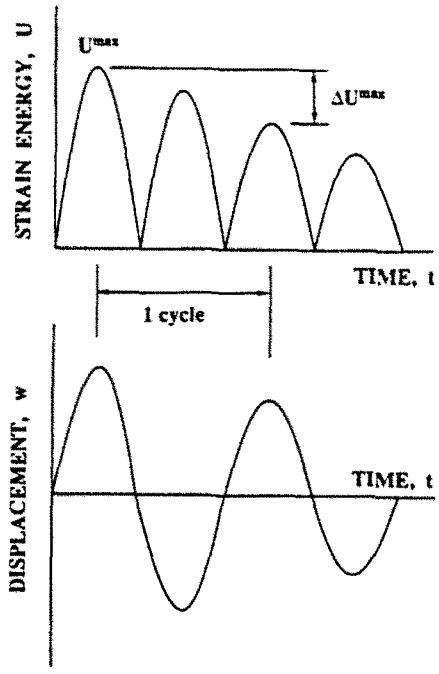

Fig. 5. Illustration of the terms used in the definition of the damping factor.

(1) either the membrane stress resultants or the membrane displacements, and
(2) either the moment resultants or the rotations, and
(3) either the transverse shear stress resultants or the normal displacement, and
(4) either the higher-order resultants or the higher-order displacement measures; these resultants ($L^{\gamma\beta}$ and $P^{\alpha\beta}$) and the displacement measures ψ_α have no ready physical interpretation.

Solutions to the equations in Table 4 can be obtained by numerical methods. These solutions provide the displacements at every point on the midsurface. Once the displacements of the midsurface are known, the displacements at any point in the shell can be determined by eqns (15) and (22). The numerical method used for obtaining solutions to the free vibration problem is discussed in Section 4.

3.5. *Damping*

The damping associated with a given mode of vibration of the shell is characterized by a modal damping factor η (also called the loss factor) defined as (Lazan, 1968)

$$\eta = \frac{\Delta U^{max}}{2\pi U^{max}}. \tag{39}$$

Here η is a measure of the strain energy dissipated per radian of vibration in the mode of interest, U^{max} the total strain energy of the entire laminate at maximum displacement during one cycle of vibration in the mode of interest, and ΔU^{max} the strain energy dissipated in that mode of vibration during the same cycle (Fig. 5). Proceeding in a manner similar to Lin *et al.* (1984), for a laminate consisting of N plies, we can write

$$U^{max} = \sum_{n=1}^{N} U_n^{max} \tag{40}$$

where U_n^{max} is the strain energy of the nth ply at the maximum displacement during one cycle of vibration in the mode of interest. Similarly, the strain energy dissipated by the laminate during the same cycle of vibration in the mode of interest is

$$\Delta U^{\max} = \sum_{n=1}^{N} \Delta U_n^{\max} \tag{41}$$

where $\Delta U_n^{\max}$ is the strain energy dissipated by the nth ply during this cycle of vibration in the mode of interest. With reference to eqn (34), the strain energy for an orthotropic ply, in terms of the ply coordinates, is

$$\begin{aligned} U_n &= \int_{V_n} \hat{U}_n \, \mathrm{d}V_n \\ &= \int_{V_n} (\tfrac{1}{2}Q_{xx}e_x^2 + \tfrac{1}{2}Q_{yy}e_y^2 + Q_{xy}e_x e_y + 2Q_{yz}e_{yz}^2 + 2Q_{xz}e_{xz}^2 + 2Q_{ss}e_{xy}^2)_n \, \mathrm{d}V_n \end{aligned} \tag{42}$$

where Q_{xx}, Q_{yy}, Q_{xy}, Q_{yz}, Q_{xz}, and Q_{ss} are the components of the reduced stiffness matrix (Jones, 1975), e_x, e_y, e_{xy}, e_{xz}, and e_{yz} the strain components (physical coefficients of the strain tensor), and V_n the ply volume. The coordinates x and y are in the directions parallel and transverse to the fibers in the plane of the ply, and z is in the direction normal to the plane of the ply. The subscript ss represents shear. From eqn (42), the maximum strain energy during one cycle of vibration can be written as

$$U_n^{\max} = (U_1 + U_2 + U_3 + U_4 + U_5 + U_6)_n^{\max} = \sum_{i=1}^{6} (U_i)_n^{\max}. \tag{43}$$

The loss of strain energy of the nth orthotropic ply is written as (see eqn (43))

$$\Delta U_n^{\max} = (\Delta U_1 + \Delta U_2 + \Delta U_3 + \Delta U_4 + \Delta U_5 + \Delta U_6)_n^{\max} = \sum_{i=1}^{6} (\Delta U_i)_n^{\max}. \tag{44}$$

Each of the six terms in eqn (44) represents the change in the strain energy associated with U_1 through U_6 during one cycle.

Analogous to eqn (39), for the nth ply a damping factor is now defined for each of the six strain energy terms

$$(\eta_i)_n = \left(\frac{\Delta U_i^{\max}}{2\pi U_i^{\max}}\right)_n, \quad i = 1, 2, \ldots, 6. \tag{45}$$

$U_i^{\max}$ is the strain energy at maximum displacement and $\Delta U_i^{\max}$ the corresponding strain energy dissipated during the ensuing one cycle of vibration.

By combining eqns (39)–(45) we obtain for each vibration mode of interest the modal damping factor for the laminate

$$\eta = \frac{\sum_{n=1}^{N} \sum_{i=1}^{6} (\eta_i (U_i)_n^{\max}}{\sum_{n=1}^{N} \sum_{i=1}^{6} (U_i)_n^{\max}}. \tag{46}$$

For each mode of vibration, the strains needed to calculate the strain energies are given by the free vibration solution of the equations of motion described in the previous subsection. The damping factors η_i must be measured experimentally.

4. METHOD OF SOLUTION

A finite element procedure was developed to obtain solutions to the equations described in the previous section. In the finite element formulation 4-node bilinear quadrilateral

elements were used. For these elements we may use seven degrees of freedom per node corresponding to the seven displacement measures (v_1, v_2, β_1, β_2, ψ_1, and ψ_2 in eqn (22) and w in eqn (16)), or we may use five degrees of freedom per node corresponding to the five displacement measures (v_1, v_2, β_1, and β_2 in eqn (23) and w in eqn (16)).

We developed an algorithm for obtaining numerical results for problems involving plates, cylindrical shells, and cylindrical panels, with or without circular cutouts. In this algorithm the entries in the element stiffness and mass matrices are evaluated by Gaussian integration schemes (Hughes, 1987). Two such schemes were built into the algorithm: the four-point (2×2) Gaussian integration scheme, and the one-point Gaussian integration scheme. To minimize errors in plates (caused by shear locking), the entries in the element stiffness matrix associated with transverse shear stiffnesses were evaluated using the one-point Gaussian integration scheme. To minimize errors in the shells (caused by shear and membrane locking), the entries in the element stiffness matrix associated with transverse shear and membrane stiffnesses were evaluated using the one-point integration scheme (selective reduced integration (SRI) or $\bar{B}$-method (Hughes, 1987). For further details of the finite element formulation the reader is referred to Bicos (1987).

We developed a computer code (designated as "VIBR8") to implement the algorithm described above. This code can be used to calculate the natural frequencies, mode shapes, and damping factors of composite plates, cylinders, and cylindrical panels with and without circular cutouts. The code was written in Fortran-77, and may be obtained from the authors. A "user-friendly" input interface allows the complete input data file to be generated in a few (5–10) minutes. Depending on the size of the problem (i.e. the number of elements used and the number of modes required on a VAX 11/780) the CPU time ranges from a few minutes for small problem (10 elements, 5 modes) to 1 h for a large problem (400 elements, 15 modes).

5. VERIFICATION OF THE MODEL

The model, the algorithm, and the computer code developed during the course of this study must be verified. This verification was effected by comparing the results of the present method to existing analytical, numerical, and experimental results pertaining to free vibration of isotropic or composite plates and cylindrical shells with or without cutouts. The problems included in our verification studies were grouped into three major categories:

(1) isotropic material: free undamped vibration;
(2) composite material: free undamped vibration;
(3) composite material: free damped vibration.

Problems related to the free *undamped* vibration of isotropic and composite materials are examined below. The free *damped* vibration of composite plates and shells will be discussed in a forthcoming paper (Bicos and Springer, 1989). The results presented were computed with five degrees of freedom per mode, using the material properties in Table 5. Materials 1 and 2 given in this table are fictitious orthotropic materials. Following the accepted custom, in the frequency vs mode number plots, the natural frequencies calculated at discrete modes are connected by continuous lines.

5.1. *Isotropic material: free undamped vibration*

The free undamped vibration of isotropic plates and shells containing no cutouts has been widely investigated (Leissa, 1969, 1973). Here we chose three problems against which to compare our results, namely, the free undamped vibration of a plate, a cylinder, and a cylindrical panel.

The first problem examined was an aluminum plate with free edges (Fig. 6). The first four natural frequencies calculated by the present method are compared with the results of the classical thin plate theory (Iguchi, 1953). There is excellent agreement between the numerical results of the present method and the analytical results of the classical plate theory.

Table 5. Material properties used in the calculations

Property	Symbol	Units	Aluminum	Steel	"Aragonite"	Material 1	Material 2	HT-S/DX210 graphite-epoxy	AVCO 5505 boron-epoxy	E-glass-epoxy
Longitudinal modulus	E_1	msi†	9.9	26	21	10	10	16.3	30	2.08
Transverse modulus	E_2	msi			11	0.4	0.25	1.14	2.7	0.74
Longitudinal shear modulus	G_{12}	msi			6.1	0.2	0.15	0.649	0.65	0.27
Transverse shear modulus	G_{23}	msi			3.7	0.2	0.15	0.649	0.65	0.27
Transverse shear modulus	G_{13}	msi			6.2	0.08	0.125	0.438	1.05	0.10
Longitudinal Poisson's ratio	ν_1	—	0.3	0.3	0.44	0.25	0.25	0.3	0.28	0.35
Density	ρ	10^{-3} lb s^2 in.$^{-4}$	0.254	0.729	1000	10000	10000	0.143	0.193	0.129

† 10^6 lb/in^2.

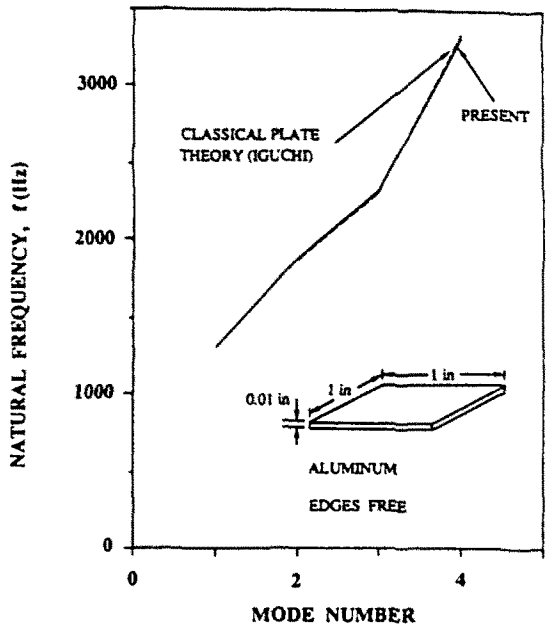

Fig. 6. Natural frequencies of a free square aluminum plate. Comparison of the results of the present method with the classical plate theory solution of Iguchi (1953).

The second problem studied was an aluminum cylinder clamped at one end (Fig. 7). We compared the natural frequencies calculated by our method with the analytical results of Resnick and Dugundji (1966). The frequencies calculated by the two methods are within 5% of each other.

The third problem considered was a steel cylindrical panel with the straight edges free and with the curved edges simply supported (Fig. 8). The natural frequencies calculated by the present method agree with the experimental data of Heki, as quoted by Leissa (1973).

Just as for the problem of plates and shells containing no cutouts, there is a considerable amount of information on the free undamped vibration of isotropic plates and shells containing cutouts (Leissa, 1969, 1973). In many of the previous reports either the results were not given in sufficient detail to be useful in comparisons, or the cutouts were rectangular (Brogan *et al.*, 1969; Aksu and Ali, 1976; Ali and Atwal, 1980; Joga-Rao and Pickett, 1961). We found two previous results that could readily be compared with our method. These were the data of Takahashi (1958) and Toda and Komatsu (1977).

Takahashi measured the fundamental frequencies of aluminum plates containing circular cutouts varying in diameter from 0 to 3.6 in. (Fig. 9). Comparisons between the

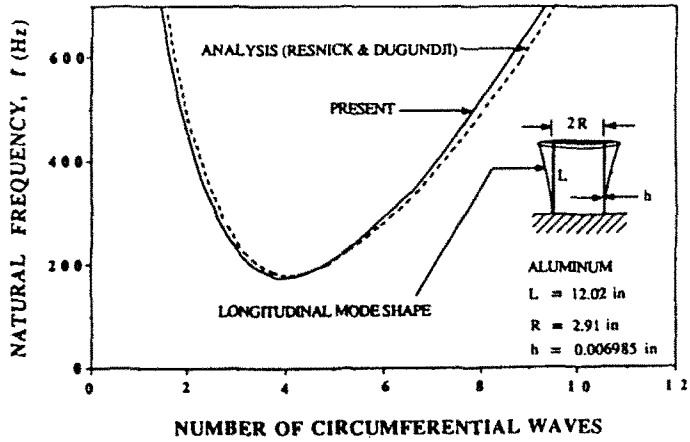

Fig. 7. Natural frequencies of an aluminum cylinder clamped along one edge and free along the other edge. Comparison of the results of the present method with the analytical results of Resnick and Dugundji (1966).

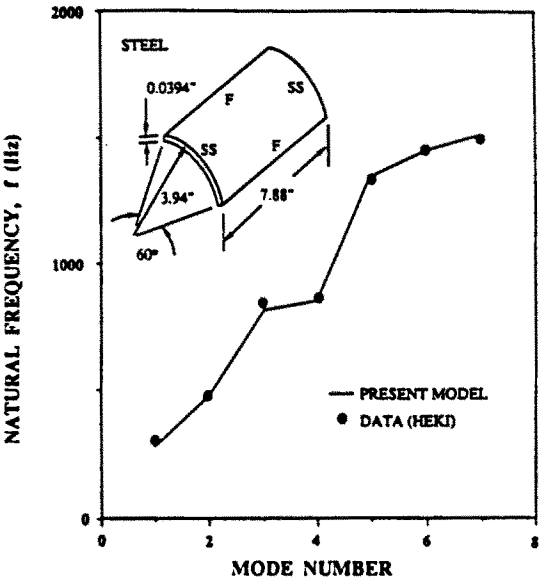

Fig. 8. Natural frequencies of a steel cylindrical panel free (F) along the straight edges and simply supported (SS) along the curved edges. Comparison of the present method for undamped vibration with the data of Heki (Leissa, 1973).

present method and Takahashi's data show good agreement, especially at smaller cutout sizes ($R/a < 0.1$). Even at larger cutout sizes the model agrees with the data within 4%.

Toda and Komatsu measured the natural frequencies of aluminum cylinders clamped along one edge. Each cylinder contained two circular cutouts located at mid-length on opposite sides of the cylinder (Fig. 10). The data of Toda and Komatsu are compared with the results of the present method in Fig. 10. The numerical results of the present method agree with the data extremely well for the first four modes. The agreement is slightly less for mode 5, but the numerical results are still within about 6% of the data.

5.2. *Composite material: free undamped vibration*

The problem of free undamped vibration of composite plates and shells has been studied widely, mostly by analytical means. For solid plates (i.e. no cutouts) we compared

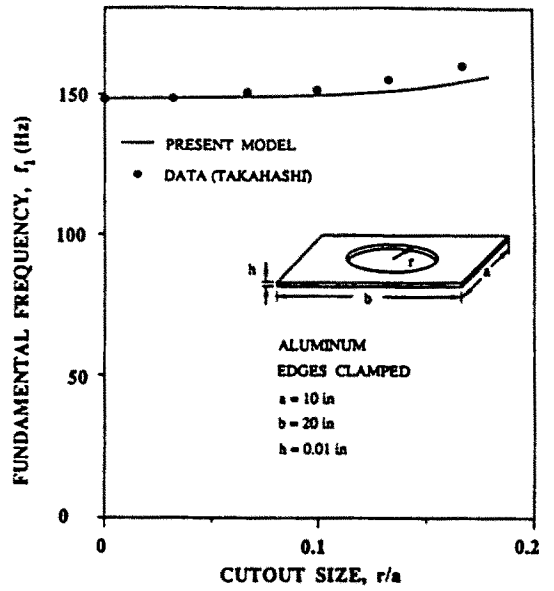

Fig. 9. Fundamental frequency as a function of cutout size of a rectangular aluminum plate with its edges clamped. Comparison of the present method for undamped vibration with the data of Takahashi (1958).

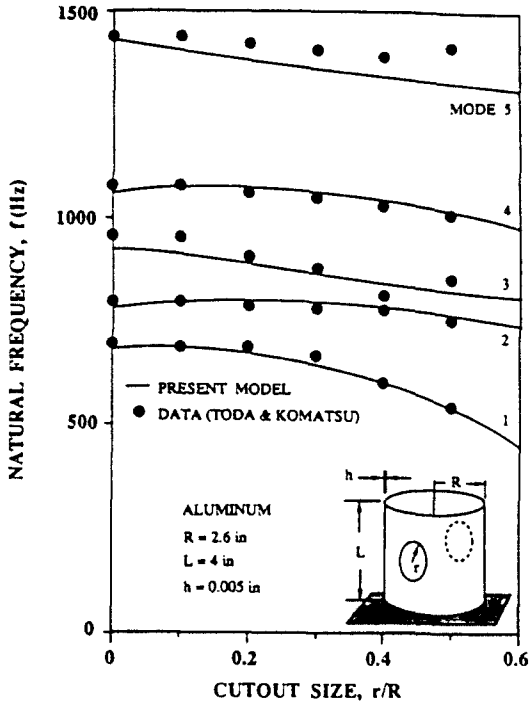

Fig. 10. Natural frequencies as a function of cutout size of an aluminum cylinder clamped along one edge and free along the other edge. There are two cutouts on opposite sides of the cylinder. Comparison of the present method for undamped vibration with the data of Toda and Komatsu (1977).

results of our model with the results of the thin plate theory of Reddy (1984) and Phan and Reddy (1985), with the results of the three-dimensional theory of elasticity as presented by Noor (1972) and by Srinivas and Rao (1970), and with the analytical results and data of Cawley and Adams (1978). For plates with cutouts we compared our results with those of Prabhakaran and Rajamani (1978). For cylinders we compared the results of our model with the numerical results of Sheinman and Grief (1984).

First, we examined two [0/90], orthotropic composite plates with their edges simply supported (Figs 11 and 12). The fundamental frequencies of these plates were calculated as a function of the modulus ratio (E_1/E_2) by the present method, and were compared with:

(1) the results of the classical thin plate theory (Phan and Reddy, 1985);
(2) the numerical results of Phan and Reddy (1985);
(3) the three-dimensional theory of elasticity given by Noor (1972).

The fundamental frequencies given by the classical plate theory are evidently in error (Fig. 11). The fundamental frequencies calculated by the present method, by the numerical procedure of Phan and Reddy, and by the three-dimensional elasticity results of Noor agree very closely over a wide range of the modulus ratio (Fig. 12).

Note that the results of Phan and Reddy were based on a "higher-order" theory using seven degrees of freedom per node. The present results computed using only five degrees of freedom per node ("standard" theory) agree very closely with the seven degrees of freedom "higher-order" theory of Phan and Reddy.

Second, we considered a square [0/45/−45/90], orthotropic composite plate with its edges clamped (Fig. 13), and calculated the fundamental frequencies as a function of the plate's length to thickness ratio. The fundamental frequencies obtained by the present method were compared with the numerical results of Phan and Reddy (1985). It is noteworthy that the "standard" theory (five degrees of freedom per node) results agree very closely with the results of the "higher-order" theory (seven degrees of freedom per node), especially when the plate is "thin" (say $L/h > 40$). This is expected since one of the assumptions in our analysis is that the thickness h is small compared to the other dimensions.

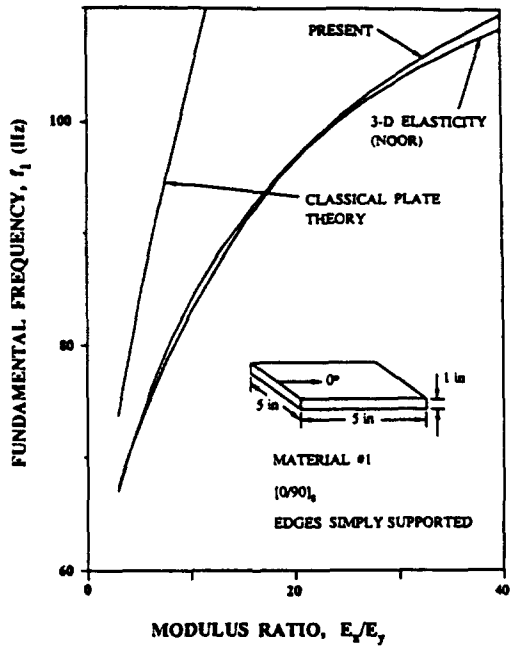

Fig. 11. Fundamental frequency of a simply supported square composite plate made of orthotropic layers. Comparison of the results of the present method with the three-dimensional elasticity results of Noor (1972) and the classical plate theory results of Phan and Reddy (1985). Material properties given in Table 5.

We studied a single layer orthotropic aragonite plate with its edges simply supported (Fig. 14). The natural frequencies calculated by the present method were compared with the natural frequencies given by the three-dimensional theory of elasticity solution presented by Srinivas and Rao (1970) and by the classical plate theory solution of Phan and Reddy (1985). The natural frequencies obtained by the present method again agree well with the

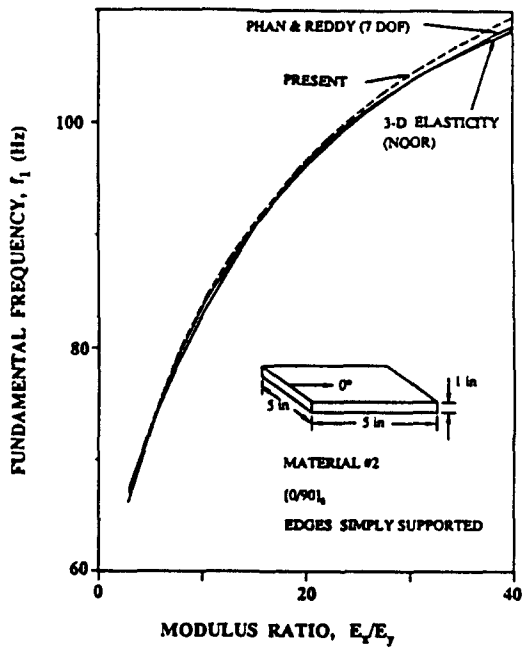

Fig. 12. Fundamental frequency of a simply supported square composite plate. Results were calculated by the present model using five degrees of freedom per node. Comparison of the present results with the numerical results of Phan and Reddy (1985) and the analytical results of Noor (1972). Material properties given in Table 5.

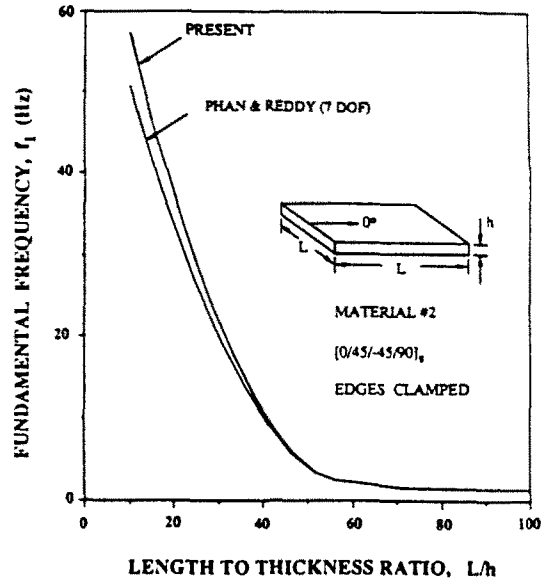

Fig. 13. Fundamental frequency of a square composite plate having its edges clamped. Comparison of the results of the present method, using the "standard" theory (five degrees of freedom per node), with the results of the "higher-order" theory (seven degrees of freedom per node) of Phan and Reddy (1985). Material properties given in Table 5.

results of the three-dimensional elasticity approach but are in disagreement with the results of the classical plate theory.

Two additional composite square plates were analyzed, with $[(45/-45)_2]_s$ and $[0/60/30/90]_s$ layups. The natural frequencies of these plates calculated by the present method were compared with the analytical results and data of Cawley and Adams (1978). There is excellent agreement between the results of the present method and the data of Cawley and Adams (Fig. 15).

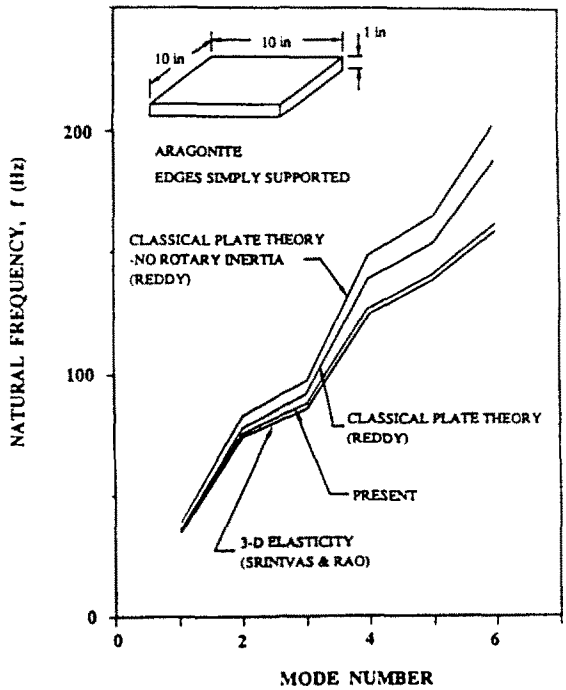

Fig. 14. Natural frequencies of a square aragonite plate with simply supported edges. Comparison of the results of the present method with the three-dimensional elasticity results of Srinivas and Rao (1970) and the classical plate theory results of Reddy (1984). Material properties given in Table 5.

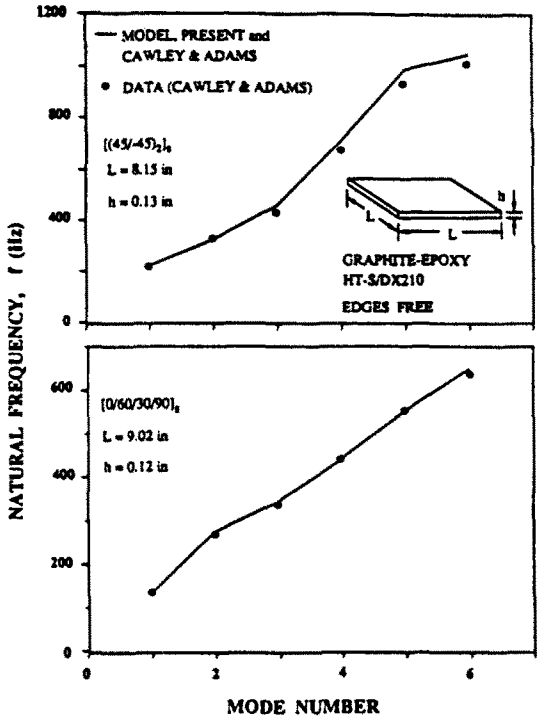

Fig. 15. Natural frequencies of graphite-epoxy plates with free edges. Comparison of the results of the present method for undamped vibration with the analysis and data of Cawley and Adams (1978). Material properties given in Table 5.

Free undamped vibration of plates with cutouts has been investigated by Lee *et al.* (1987) and by Prabhakaran and Rajamani (1978). The analysis of Lee *et al.* (1987) applies to plates with rectangular cutouts, hence their results could not be compared with ours. Prabhakaran and Rajamani calculated the natural frequencies of clamped unidirectional composite plates containing a circular cutout. We compared the results of the present

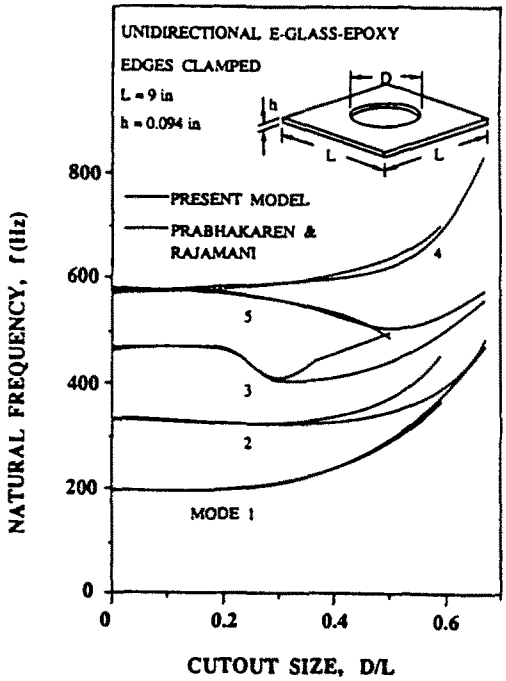

Fig. 16. Natural frequencies as a function of cutout size of a unidirectional E-glass-epoxy plate with its edges clamped. Comparison of the results of the present method with the analytical results of Prabhakaran and Rajamani (1978). Material properties given in Table 5.

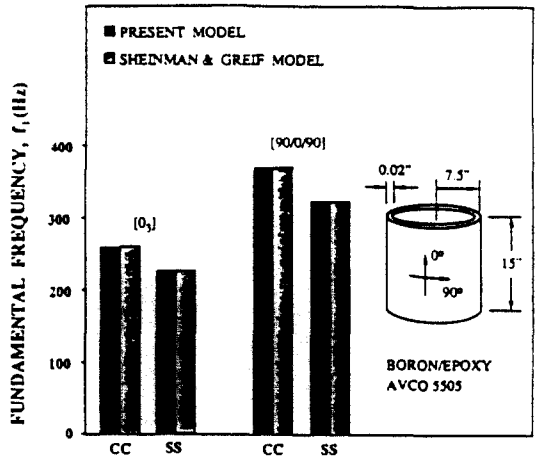

Fig. 17. Fundamental frequencies of two boron-epoxy cylinders made of unidirectional $[0_3]$ and cross-ply [90/0/90] laminates. The edges of the cylinders are either clamped (CC) or simply supported (SS). Comparison of the results of the present method with the numerical results of Sheinman and Greif (1984). Material properties given in Table 5.

method with those given by Prabhakaran and Rajamani for a 9 in. square, 0.094 in. thick clamped plate made of undirectional E-glass-epoxy (Fig. 16). The natural frequencies calculated by the present method agree well with those of Prabhakaran and Rajamani.

In addition to composite plates, we also applied the model to the problem of free undamped vibration of a composite cylinder made of three boron-epoxy plies, arranged as either $[0_3]$ or [90/0/90]. The edges of the cylinder were either clamped (CC) or simply supported (SS). The fundamental frequencies calculated by the present method and by Sheinman and Grief (1984), are within 1% (Fig. 17).

6. CONCLUDING REMARKS

The equations presented in this paper describe the free damped vibrational characteristics of laminated fiber-reinforced composite plates and shells. The "VIBR8" computer code applies to rectangular plates, cylinders, and cylindrical panels, which may contain one or two symmetrically located circular cutouts. However, by using the equations developed in this study, the code could readily be extended to other shell geometries.

We note that the computer code can be used to analyze both the free damped and undamped vibration of flat and cylindrical panels made of fiber-reinforced organic matrix composites. The code should not be applied to the free damped vibration of such panels made of an isotropic material because the assumption used in the analysis, that damping is independent of frequency, generally is invalid for isotropic materials. Since this assumption does not affect the results for free undamped vibration, the code may also be used to study the free undamped vibration of rectangular plates, cylinders, and cylindrical panels made of an isotropic material or alternating layers of isotropic and composite materials.

REFERENCES

Aksu, G. and Ali, R. (1976). Determination of dynamic characteristics of rectangular plates with cutouts using a finite difference formulation. *J. Sound Vibr.* **44**(1), 147–158.

Alam, N. and Asnani, N. T. (1984a). Vibration and damping analysis of a multilayered cylindrical shell, Part I: theoretical analysis. *AIAA J.* **22**(6), 803–810.

Alam, N. and Asnani, N. I. (1984b). Vibration and damping analysis of a multilayered cylindrical shell, Part II: numerical results. *AIAA J.* **22**(7), 975–981.

Alam, N. and Asnani, N. T. (1986). Vibration and damping analysis of fibre-reinforced composite material plates. *J. Composite Mater.* **20**(1), 2–18.

Alam, N. and Asnani, N. T. (1987). Vibration and damping analysis of fibre-reinforced composite material cylindrical shell. *J. Composite Mater.* **21**(4), 348–361.

Ali, R. and Atwal, S. J. (1980). Prediction of natural frequencies of vibration of rectangular plates with rectangular cutouts. *Comput. Struct.* **12**(6), 819–823.

Bicos, A. S. (1987). Free damped vibration of composite plates and shells. Ph.D. thesis, Stanford University.

Bicos, A. S. and Springer, G. S. (1989). Free damped vibration of composite plates, cylinders and cylindrical panels with cutouts. *AIAA J.* (in press).

Brogan, F., Forsberg, K. and Smith, S. (1969). Dynamic behavior of a cylinder with a cutout. *AIAA J.* **7**(5), 903–911.

Cawley, P. and Adams, R. D. (1978). The predicted and experimental natural modes of free-free CFRP plates. *J. Composite Mater.* **12**(5), 336–347.

Flugge, W. (1972). *Tensor Analysis and Continuum Mechanics*, Chap. 1. Springer, New York.

Hughes, T. J. R. (1987). *The Finite Element Method*, Chaps 1 and 6. Prentice-Hall, Englewood Cliffs, New Jersey.

Iguchi, S. (1953). Die Eigenschwingungen und Klangfiguren der Vierseitig Freien Rechteckigen Platte. *Ing. Arch.* **21**, Ser. 303, No. 5–6, 304–322.

Joga-Rao, C. V. and Pickett, G. (1961). Vibrations of plates of irregular shapes and plates with holes. *J. Aeronaut. Soc. India* **13**(3), 83–88.

Jones, R. M. (1975). *Mechanics of Composite Materials*, Chap. 4. Scripta, Washington, DC.

Lazan, B. J. (1968). *Damping of Materials and Members in Structural Mechanics*, pp. 30–32. Pergamon Press, Oxford.

Lee, H. P., Lim, S. P. and Chow, S. T. (1987). Free vibration of composite rectangular plates with rectangular cutouts. *Composite Struct.* **8**(1), 63–81.

Leissa, A. W. (1969). Vibration of plates, NASA SP-160.

Leissa, A. W. (1973). Vibration of shells, NASA SP-288.

Lin, D. X., Ni, R. G. and Adams, R. D. (1984). Prediction and measurement of the vibrational damping parameters of carbon and glass fibre-reinforced plastics plates. *J. Composite Mater.* **18**(2), 132–152.

Meirovitch, L. (1967). *Analytical Methods in Vibrations*, pp. 42–45. Macmillan, New York.

Naghdi, P. M. (1963). Foundations of elastic shell theory. In *Progress in Solid Mechanics* (Edited by I. N. Sneddon and R. Hill), Vol. IV, Chap. 1. North-Holland, Amsterdam.

Naghdi, P. M. (1984). The theory of shells and plates. In *Mechanics of Solid* (Edited by C. Truesdell), Vol. II, pp. 425–640. Springer, New York.

Ni, R. G. and Adams, R. D. (1984). The damping and dynamic moduli of symmetric laminated composite beams—theoretical and experimental results. *J. Composite Mater.* **18**(2), 104–121.

Noor, A. K. (1972). Free vibrations of multilayered composite plates. *AIAA J.* **11**(7), 1038–1039.

Phan, N. D. and Reddy, J. N. (1985). Analysis of laminated composite plates using a higher-order shear deformation theory. *Int. J. Numer. Meth. Engng* **21**(12), 2201–2219.

Prabhakaran, H. and Rajamani, A. (1978). Free vibration characteristics of clamped clamped composite plates with circular holes and square cutouts. *Proceedings of the International Conference on Composite materials 2nd (ICCM2)*, pp. 367–375. Metallurgical Society of AIME, Warrendale, Pennsylvania.

Reddy, J. N. (1984). *Energy and Variational Methods in Applied Mechanics*, pp. 364–382. Wiley, New York.

Resnick, B. S. and Dugundji, J. (1966). Effects of orthotropicity, boundary conditions, and eccentricity on the vibrations of cylindrical shells. Air Force Office of Scientific Research, Scientific Report AFOSF 66-2821, ASRL TR 134-2 (AD648 077).

Sheinman, I. and Grief, S. (1984). Dynamic analysis of laminated shells of revolution. *J. Composite Mater.* **18**(3), 200–215.

Srinivas, S. and Rao, A. K. (1970). Bending, vibration and buckling of simply supported thick orthotropic rectangular plates and laminates. *Int. J. Solids Structures* **6**(11), 1463–1481.

Takahashi, S. (1958). Vibration of rectangular plates with circular holes. *Bull. JSME* **1**(4), 380–385.

Toda, S. and Komatsu, K. (1977). Vibrations of circular cylindrical shells with cutouts. *J. Sound Vibr.* **52**(4), 497–510.

Tsai, S. W. and Hahn, H. T. (1980). *Introduction to Composite Materials*, pp. 217–239. Technomic, Westport, Connecticut.